Microsystems for cell-based electrophysiology



2013 J. Micromech. Microeng. 23 083002

(http://iopscience.iop.org/0960-1317/23/8/083002)

IOP PUBLISHING JOURNAL OF MICROMECHANICS AND MICROENGINEERING

J. Micromech. Microeng. **23** (2013) 083002 (16pp) doi:10.1088/0960-1317/23/8/083002

TOPICAL REVIEW

# Microsystems for cell-based electrophysiology

**Levent Yobas**

Department of Electronic and Computer Engineering, The Hong Kong University of Science and Technology, Clear Water Bay, Kowloon, Hong Kong

E-mail: eelyobas@ust.hk

Received 23 January 2013, in final form 22 April 2013
Published 3 July 2013
Online at stacks.iop.org/JMM/23/083002

**Abstract**

Among the electrophysiology techniques, the voltage clamp and its subsequent scaling to smaller mammalian cells, the so-called patch clamp, led to fundamental discoveries in the last century, revealing the ionic mechanisms and the role of single-ion channels in the generation and propagation of action potentials through excitable membranes (e.g. nerves and muscles). Since then, these techniques have gained a reputation as the gold standard of studying cellular ion channels owing to their high accuracy and rich information content via direct measurements under a controlled membrane potential. However, their delicate and skill-laden procedure has put a serious constrain on the throughput and their immediate utilization in the discovery of new cures targeting ion channels until researchers discovered 'lab-on-a-chip' as a viable platform for the automation of these techniques into a reliable high-throughput screening functional assay on ion channels. This review examines the innovative 'lab-on-a-chip' microtechnologies demonstrated towards this target over a period of slightly more than a decade. The technologies are categorically reviewed according to their considerations for design, fabrication, as well as microfluidic integration from a performance perspective with reference to their ability to secure G Ω seals (gigaseals) on cells, the norm broadly accepted among electrophysiologists for quality recordings that reflect ion-channel activity with high fidelity.

(Some figures may appear in colour only in the online journal)

## 1. Introduction

Ion channels, pore-forming proteins, reside across the cell membrane, which is a phospholipid bilayer impermeable to ions, and actively regulate the exchange of ions, often exclusive to a specific type [1]. Their role in electrically excitable tissues such as nerves and muscles are relatively well understood, particularly the crucial role of the voltage-gated $Na^+$ and $K^+$ channels in mediating membrane depolarization and repolarization during the generation and propagation of action potentials. Mutations in these channels could impair transduction of rapid electrical signalling and thus adversely affect brain, muscle and sensory functions. Yet relatively less understood is the role of ion channels in non-excitable tissues (beyond nerves and muscles) such as the regulation of blood pressure, salt and water balance, lymphocyte proliferation, fertilization and cell death [2]. The fact that a broad spectrum of diseases, e.g. epilepsy, diabetes, migraine, myotonia, cardiac arrhythmia, may be treated with the modulators of ion channels makes them a viable therapeutic target and calls for effective high-throughput assays to screen libraries of potential drug candidates on ion channels [3, 4].

Indirect assays, such as those using fluorescent dyes to probe the consequent change in the membrane potential or those tracking the movement of radioactive isotopes of ions, trade data quality for throughput and consequently inherit serious drawbacks such as the lack of precision, lack of control over membrane potential, low fidelity, low sensitivity and low temporal resolution [5–7]. Moreover, functional cell-based indirect assays are mostly homogenous with the

 

recordings averaged across a large population of cells. Indirect measurements of the ion-channel activity do not correlate well with those from electrophysiological recordings, demanding a continued reliance on the latter for a confirmation of the compound activity and efficacy. This poses a considerable bottleneck in drug discovery. All these shortcomings put these assays vulnerable to false negatives; a high-quality compound could be missed out due to masking of important pharmacological interactions between drug compounds and ion channels.

Regarded as the gold standard, patch clamp is the only technique that allows for direct measurements of the effect of active compounds on the kinetics of ion channels in real-time and ultra-high resolution ($<1\mu$s and $<1$pA) while maintaining a tight control over the membrane potential [8, 9]. The measurements offer unequalled information content regarding the channel function, kinetics, gating, pharmacology and desensitization. Patch clamp in its traditional form is an extremely laborious and skill-laden craft that may take years to master. It requires a skilled scientist to manoeuvre a heat-polished highly tapered tip of a freshly pulled glass micropipette, $\sim 1\mu$m in opening diameter, with such a high precision that the tip can be brought as near as possible to the cell of interest adhered to a solid support, see figure 1(*a*). At the disposal of the scientist is a sophisticated setup to aid the process including a precision micromanipulator and a powerful optical microscope to be placed on a vibration-isolation table while enclosed by a faraday cage to shield electromagnetic interference. Guided by the monocular vision of the microscope optics, the scientist is often challenged by the lack of depth perception, which makes it hard to judge the relative position of the tip of the micropipette with respect to the cell.

Once near the cell, a mild suction is applied through the micropipette to pull a portion of cell membrane into the tip without damaging the cell and upon which an electrically and mechanically tight seal spontaneously forms between the cell membrane and the interior of the micropipette, figure 1(*b*). This tight seal, typically in the order of GΩ, is referred to as 'gigaseal' and sets the signal quality for resolving weak ionic currents in the range of picoamperes (pA). Subsequently, according to the specific mode of the technique employed, the scientist either retracts the micropipette tip and, along with it, detaches the patch of the membrane from the cell without losing the seal (excised-patch mode), figure 1(*c*), or applies a brief pulse of suction or a zap of voltage to break open the membrane patch and gain electrical access to the cell interior (whole-cell mode), figure 1(*d*). A pair of chlorinated silver wires (Ag/AgCl) as the recording and reference electrodes is immersed in the electrolyte (intracellular) solution that fills the micropipette and in the bath (extracellular) solution surrounding the tip, respectively. Both the recording and reference electrodes are connected to the headstage unit of a patch clamp amplifier for processing and displaying ionic currents. While the method is capable of recording from a single-ion channel that happens to be isolated within an excised patch of cell membrane, whole-cell configuration is of greater significance for identifying the functional relevance

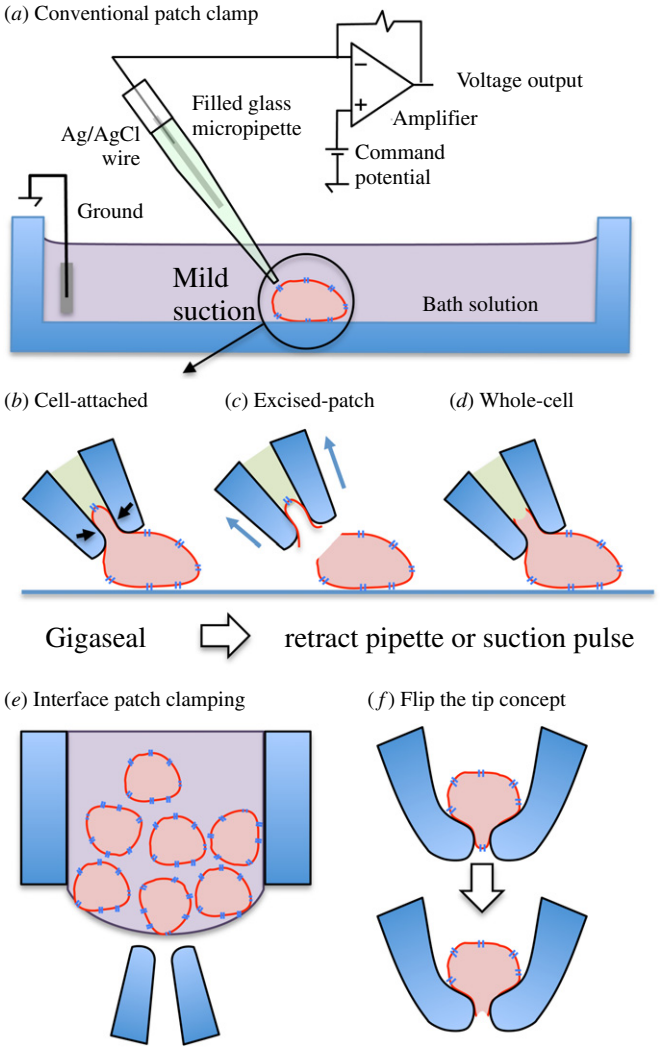


**Figure 1.** Cross-sectional schematics describing patch clamp technique. (*a*) Conventional approach as routinely performed utilizing a glass micropipette electrode on a cell adhered to a solid support arranged in various recording configurations: (*b*) cell-attached, (*c*) excised-patch and (*d*) whole-cell mode. 'Blind' approaches where the configuration is inverted and a cell is rather approached to the micropipette opening and probed or patched in suspension in an effort to automate the technique. (*e*) Interface patch clamping relies on precision manoeuvring of a cell suspended near the air–liquid interface to the tip of an inverted micropipette blindly based on the electrical resistance reading across the tip and (*f*) flip-the-tip uses suction or gravitational forces to position a cell suspended inside the pipette tip.

of the action of a compound and thus more preferred by the pharmaceutical companies.

Earlier efforts to automate the laborious patch clamp technique for increased throughput replaced the skilled operator with a robotic system equipped with computer vision and capable of navigating a micropipette electrode, locating and patching a cell [10]. Robotic systems have also been developed to automate two electrode voltage clamp, a related technique yet far less stringent in its precision requirement, since it is performed on sufficiently large cells like oocytes nearly 1 mm in diameter [11, 12]. Still, the systems adopting this automation strategy continued to rely on conventional

glass micropipettes and as a result could only achieve a limited throughput. Interface patch clamping is perhaps the first 'blind' patch clamping method that has abandoned the machine vision and rather precision manipulated a capillary tube which presents a hanging drop of cells to the tip of an inverted patch micropipette blindly (guided by resistance reading) to patch a random cell near the air–liquid interface, figure 1(*e*) [13–15]. A subsequent effort (flip-the-tip) has also eliminated the need for a precision manipulator by inverting the entire cell–pipette configuration by placing the cell suspension inside a micropipette tip and allowing the cell to settle towards the tip where it can be trapped and a tight seal can be established under suction or centrifugation, figure 1(*f*) [16]. The gigaseal formed with the cell inside the patch micropipette was found to be extremely durable to the extent that tapping against the micropipette wall or moving it around did not break the seal. Thus, with the 'blind' patch clamping, not only has the skilled operator become redundant but also the need for a sophisticated setup has been avoided including the precision micromanipulator, microscope, vibration-isolation table and bulky Faraday cage. The inverted configuration reflects the underlying principle of many chip-based approaches in the automation of the conventional technique: to move the cell towards a fixed microscopic aperture emulating the opening of a micropipette tip. In fact, one could trace back the idea of docking a cell to an aperture on a planar partition for whole-cell measurements to 1970s when the idea was attempted not so much as to automate the procedure but rather to establish internal perfusion or dialysis to the cell [17]. The idea was revived in the late 1990s with the availability of smaller planar patch apertures through microfabrication. Unlike the patch micropipettes, the chips as a platform do offer a great deal of advantage when it comes to scaling up the approach to a massive array since microfabrication of a single unit or an array more or less demands the same effort.

The scope of this review encompasses microfabricated devices reported thus far and their ability to form gigaseals on various types of cells. The reader can refer to some of the excellent reviews [18–24] on the topic for the early achievements in the field that are included here as well for completeness along with a series of new developments emerged in recent years. In this review, the devices are classified according to their design configurations, i.e. lateral or planar, as well as their choice of substrate materials, i.e. silicon, glass or polymer, which determines by default their fabrication process and the toolbox of technologies to draw from, i.e. etching, moulding or drilling. Microfluidic integration of the devices is briefly discussed, particularly in consideration of the planar design, for facilitating key functionalities including the cell manipulation to the patch apertures and application of compounds to the patched cells. This review neither covers cell preparation protocols, although it is well known by now that the choice of the cell protocol, including the cell type, is as crucial as the device itself in achieving gigaseals, nor does it cover a broad spectrum of existing cell manipulation techniques, i.e. dielectrophoresis [25], acoustophoresis [26] and magnetophoresis [27], which could greatly benefit the devices discussed herein. These techniques are addressed in great depth in dedicated reviews [28]. This review mostly excludes the devices with apertures built across thin insulating partitions to form artificial lipid bilayers that incorporate ion channels in a precisely defined composition of lipids as well as of surrounding electrolytes for controlled electrophysiology measurements [29, 30]. Such constructs are considered the predecessors of the devices reviewed here with research on them dates back earlier, yet such apertures are too large to be applied for patch clamping mammalian cells.

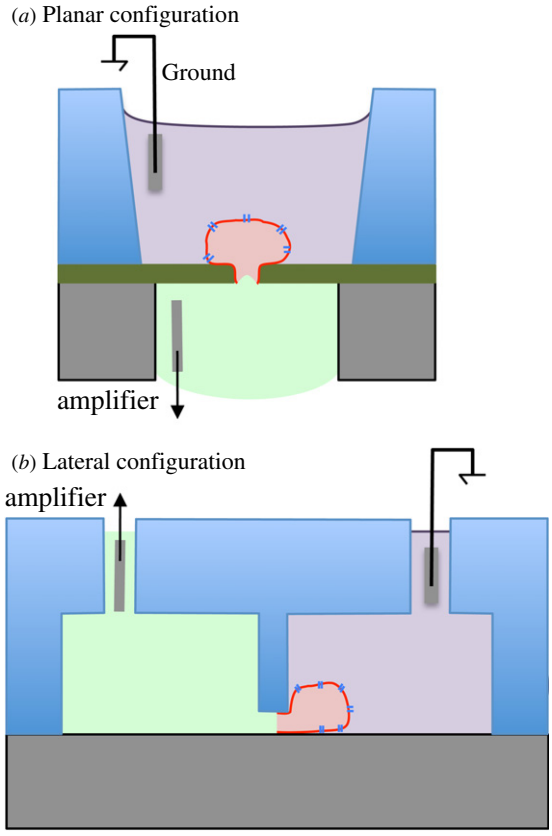


**Figure 2.** Cross-sectional schematics describing the chip-based approaches proposed to automate patch clamp (whole-cell) technique and classified here into (*a*) planar and (*b*) lateral designs.

## 2. Design considerations

### *2.1. Planar*

With very few exceptions, the design of all the chip-based devices exhibits a planar configuration whereby the microscopic aperture for probing the cell is situated on a thin dielectric partition that keeps the top cell suspension apart from the bottom recording electrolyte as described in figure 2(*a*) [31–63]. The popularity of this configuration arises from its intuitive method of fabrication based on the available techniques, which may easily supersede any other advantage it may offer. Among all, the configuration offers an open-access platform where cells and reagents can be conveniently added into individual compartments or wells from above. Such open-access platform also allows one to efficiently perfuse drugs of a specific concentration to the cell without compromising the

seal status. This task could leverage a liquid dispensing robot; the workhorse of laboratories conducting high-throughput screening assays in standard microtitre plate wells. Yet, a disadvantage of an open-access platform is that it requires a fairly dense suspension of homogenous cells that is free of particulates as the procedure relies on a random event of a cell under gravity coming to rest over the aperture where suction helps in final docking and sealing of the cell. A microfluidic channel built over the aperture may allow one to manipulate and identify a cell of interest before docking but at the expense of some of the articulated benefits of an open-access platform [35, 36].

The planar configuration is also advantageous in that it is amenable to lithography-based patterning such that the aperture geometry can be easily transferred onto an etch mask placed on the device substrate. Taking full advantage of the top-down micro/nanotechnology, one could shape the topography around the aperture and craft a three-dimensional nozzle or funnel-type structure [37], more representative of a conventional patch micropipette. A limitation of the planar configuration, however, could be the maximum achievable density of the array, when scaling up the platform, simply due to complex integration of the isolated fluidic compartments placed above and below thin dielectric partitions. Moreover, such vertical stacking may pose a further limitation if the overall device structure becomes relatively thick for high-magnification optical microscopy. This prevents one to visually assess the mechanical deformation of the cell membrane while concurrently recording ionic currents. The simultaneous mechanical and electrical characterization of single cells can be fundamental to the understanding of cell properties and correlate well with the diseases such as malaria and cancer [64].

### *2.2. Lateral*

A lateral configuration keeps a thin insulating partition between compartments situated on the same planar surface of a substrate; see figure 2(*b*) [65–73]. Thus, it avoids the requirement of etching nearly the entire thickness of the substrate so as to form the thin insulating partition that contains an aperture. Moreover, by limiting the depth of etching, the volume of each compartment can be further miniaturized. In fact, compartments turn into microchannels that can be conveniently designed on a lithographic layout. Similarly, one could register an optimized profile for the thin insulating partition between the compartments to reduce device capacitance and associated transient currents [65]. Particularly, a reduced device capacitance is of utmost importance as the device capacitance contributes to the several noise terms through the lossy dielectric of the substrate, the capacitive loading at the input of the amplifier, distributed RC noise and the noise arising from the access resistance in series with the cell membrane. Above all, lateral configuration leaves cells in sight for microscopic viewing such that one could inspect cells, choose a particular cell of interest to manipulate and capture, and then record whole-cell ionic activity while assessing both deformation and integrity of the captured cell membrane [66]. Its inherent microfluidic integration allows auxiliary apertures to be precisely located near a patch aperture without involving extra fabrication steps and these can be dedicated to cell manipulation or rapid solution exchange through suction/pressure applied through them [67, 68]. The latter is of particular significance in pulsed application of drug compounds on the patched cells to study ligand-gated ion channels and ion-channel kinetics [74]. The precision enables a very high-density array of patch apertures, each having its own dedicated access port, not only for increased throughput but also for the study of the gap junctions in cell pairs in intimate contact [75].

Many of the benefits articulated above are gained because the lithography is primarily reserved for registering the optimized profile of the insulating partition as well as the compartments rather than the aperture itself. However, this choice comes at the expense of the flexibility in defining the round patch aperture, as the aperture is no longer planar or amenable to lithographic patterning. Hence, the challenge in lateral configuration remains to be the fabrication of an ideal round patch aperture on a thin insulating partition distanced from the confining corners or boundaries of microchannnels. While such configuration has yet to be fulfilled, researchers have moved forward with non-ideal yet practical demonstrations having rectangular or quasi-round patch apertures cornered between a sidewall and the floor of a microchannel [65–67]. These apertures are typically formed at the intersection of a shallow trench profile preferably 1–2 $\mu$m in critical dimension with a deeper trench structure that can accommodate cells in suspension. Thus, the process in essence requires a substrate microstructured with a dual-step profile and then capped with a plain substrate for fluidic enclosure. Microstructuring the substrate may involve etching [69–72] or moulding [65–68, 73] as will be discussed in the following section.

## 3. Fabrication considerations

### *3.1. Silicon*

Silicon is a well-established technology owing to the advances made in microelectronics and microelectromechanical systems (MEMS) industry over the decades [76]. The technology has become more versatile with the launch of the Bosch process, which has led to microstructures with various three-dimensional (3D) profiles realized in a deep reactive ion etching (DRIE) system [77, 78]. Thus, early patch-clamp chips adopted silicon as an obvious choice, and yet, typically focused on devices with a quasi-two-dimensional (2D) profile that have posed small apertures on thin dielectric partitions, thin-film oxide or nitride membranes, suspended over silicon pits. Fertig *et al* introduced apertures with diameters down to 50 nm on thin-film $Si_3N_4$ membranes (100–200 nm) through a combination of reactive ion etching and backside KOH etching [31]. Individual cells manually positioned on these apertures increased the shunt resistance but only slightly. On the same type of structures, Schmidt *et al* applied a coating layer of a thin-film $SiO_2$ (20 nm) and then modified the surface

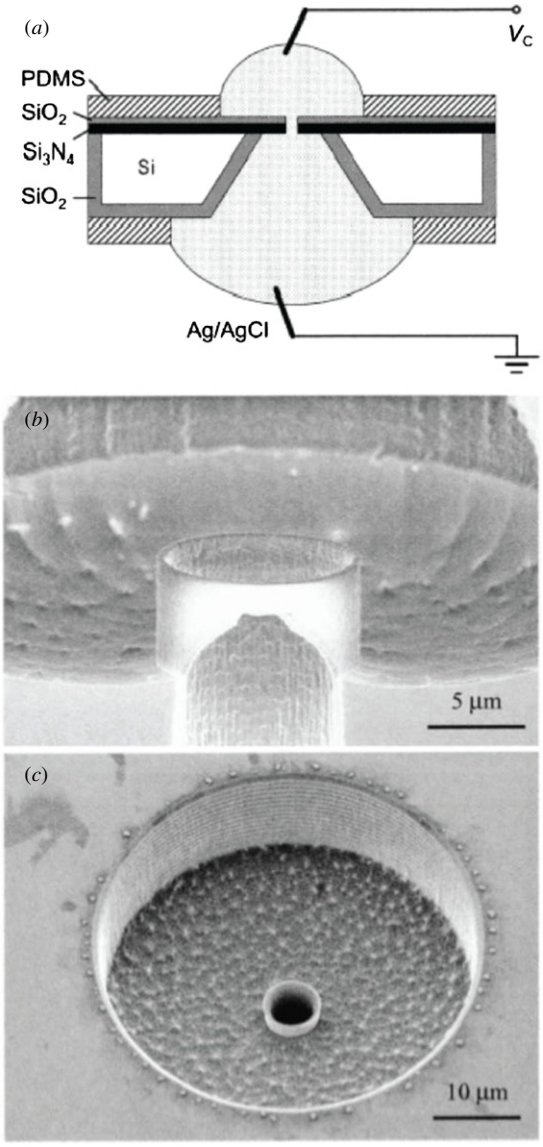


**Figure 3.** Planar designs in Si. (*a*) Illustration of a quasi-2D aperture in a $Si_3N_4/SiO_2$ membrane freestanding between compartments confined by polydimethylsiloxane (PDMS) pads. (Reprinted with permission from [32]. Copyright 2000, Wiley-VCH.) (*b*) and (*c*) Scanning electron microscope (SEM) images of 3D nozzle structures of a $SiO_2$ film protruding out of plane and in (*b*) diameter 10 $\mu$m, height 6 $\mu$m (broken open during preparation) and (*c*) diameter 4 $\mu$m. (Reprinted with permission from [37]. Copyright 2002, American Institute of Physics).

with aminosilane or poly-L-lysine to impart positive charges, figure 3(*a*) [32]. Negatively charged liposomes were shown to fuse to the chip surface under electrostatic attraction, forming stable gigaseals (1−200 GΩ) upon lipid layers suspended over the apertures. Self-positioning of liposomes on the apertures was realized under electrophoretic focusing. However, no measurement from cells has been reported using such devices.

The above studies conclude that a quasi-2D aperture profile on a dielectric membrane of a thickness well below 1 $\mu$m appears to be insufficient to form a tight seal with cell membrane unless the surface is chemically modified to promote stronger adhesion. Stett *et al* [33] described a seal resistance model that suggested a minimal contribution from cell membrane adhesion to the planar surface surrounding the aperture as opposed to aperture sidewall. Using a 2.5 $\mu$m diameter aperture defined on a relatively thick (∼2 $\mu$m) silica (thermal $SiO_2$) membrane, Sordel *et al* [34] achieved high-resistance seals on the non-transfected Jurkat cells but not on the transfected Chinese hamster ovary (CHO) cells (<100 MΩ) to enable whole-cell measurements. The authors improved on their structure by depositing a 1.5 $\mu$m thick plasma-enhanced chemical vapor deposition (PECVD) oxide film which narrowed down the aperture diameter to 1.7 $\mu$m while increasing its depth to ∼3.5 $\mu$m. The improved structure managed to form tighter seals on transfected cells (HEK-293 cells with BK-type-$Ca^{2+}$-activated channels and CHO cells with inward rectifier IRK1 channels) exceeding 100 MΩ in 50% of the trials including few occurrences of gigaseals. This is despite the fact that the PECVD oxide increased the surface roughness to nanometers range, an order of magnitude higher than that offered by the smoother silica surface underneath. The authors held the additional surface area contributed by the increased surface roughness responsible for the improved seal performance along with the 'hourglass' aperture profile arising from non-conformal coating of the PECVD film.

A further drawback of a quasi-2D aperture is the large device capacitance imposed by a thin dielectric membrane that cannot be simply cancelled out by the settings of a patch-clamp amplifier. Thus, the subsequent studies began to take advantage of DRIE process and explore various 3D apertures on a thick silicon membrane. Applying DRIE both on the front as well as on the backside of a wafer patterned through standard photolithography, Pantoja *et al* [35] obtained a high-aspect-ratio aperture 2 $\mu$m in diameter on a silicon membrane 20–40 $\mu$m thick. Conformal deposition of an insulating $SiO_2$ layer further narrowed down the aperture to a diameter of 1.5–1.8 $\mu$m. Yet, the occurrence of gigaseals was rather rare and attributed to the non-negligible roughness of the etched aperture walls. Matthews and Judy tried to rectify this issue by growing a thermal oxide layer that was shown to inherit the roughness while smoothening the underlying silicon [36]. By stripping off the oxide, they exposed the underlying smoothened silicon and grew a new thermal oxide layer with rather a smooth surface finish. They also incorporated an underlining thin layer of amorphous silicon to mitigate the faceting of the aperture that comes with the growth rate dependence of oxide on the silicon crystallographic orientation. Regrettably, the smoothening of the etched surface did not translate into an increased gigaseal success rate.

Lehnert and colleagues [37] also leveraged DRIE and sculpted hollow $SiO_2$ nozzles protruding out of plane and embedded in larger cavities, figures 3(*b*) and (*c*). The nozzles emulated the 3D profile of a patch pipette tip and their overall depth 30 $\mu$m provided sufficient contact area for seal formation. Thus, the nozzles, diameter down to 2.5 $\mu$m, returned encouraging seal resistance values (100–200 MΩ) on CHO cells immobilized by suction. As with all the etched apertures, the nozzles exhibited a rough surface (∼70 nm peak-to-peak) which was subsequently smoothened by applying a coating of a thin (<1 $\mu$m) layer of polydimethylsiloxane (PDMS) [38] or a layer of glass thermally annealed for reflow (section 3.6) [39].

Curtis *et al* [40] investigated the impact of several physical device features on seal formation more systematically in various silicon-based devices within the context of a single basic design. In their study, the smoother thermal oxide surface produced better quality seals than the rougher PECVD surface on neuroblastoma cells, disputing the finding of Sordel *et al* [34]. Yet, they found the yield of successful recordings frustratingly low with an average seal resistance 96 MΩ. They tested devices specifically with an aperture size 1.5–2.5 $\mu$m in diameter and 7–12 $\mu$m in depth, with a coating of either thermal oxide or PECVD $SiO_2$. In some devices, the thermal-oxide coatings were converted into protruding nozzle structures and in some others they were boron doped for a glassy borosilicate melt emulating the surface state of a glass patch pipette. The authors found little or no impact on the seal quality of all the physical features tested including the aperture diameter, the presence of protruding nozzle and the boron-doped surface state. Exception to those was the aperture depth with which the seal resistance was found to positively correlate. Overall, the authors managed to obtain a single gigaseal and a number of sub-gigaseals (30–250 MΩ) with whole-cell recordings that fared well with those from a conventional setup.

The intuitive notion that the seal quality must correlate with the intricate design of the aperture shape has received little or no experimental support. Although this comes as a surprise, under these circumstances, one should reflect again on the advantages offered by silicon, particularly the simplicity of sculpting (sub)micron features in this semiconducting material and weigh them against its drawbacks such as inherently large device capacitance (hundreds of picofarads), slow voltage transients and excess noise due to high density of free charge carriers present. One should also take note of the fact that even more charge carriers to be induced with exposure to light owing to the photoelectric effect. To reduce the device capacitance in silicon, one must avoid light (e.g. microscope inspection), employ a thicker dielectric coating, and minimize the electrolytic area by limiting the contact between the fluid and the substrate.

### *3.2. Quartz/glass*

Quartz/glass offers superior dielectric properties that help drastically reduce dielectric noise and capacitive transients. Single-crystal quartz and borosilicate glass has a dielectric loss factor $\sim 10^{-4}$ and $3.7 \times 10^{-3}$ while dielectric constant ~3.8 and 4.6, respectively. Quartz or glass is also the material of choice when it comes to forming gigaseals with the cell membrane [79]. Unsuccessful attempts over the patch apertures in thin-film membranes diverted the attention to quartz or glass and a method of etching a small patch aperture in them, which is known to be technically challenging. Wet etching small features in this kind of materials is a challenge since it undercuts the etch mask [80]. Dry etching minimizes any undercut but is by far less practical for glass or quartz than for silicon due to slow etch rates and rough surface finish [81]. Fertig and colleagues [41–44] took up the challenge and developed an ingenious method of ion track milling whereby a pre-thinned fused quartz or borosilicate glass is penetrated with precisely one gold ion damaging the local electronic structure, leaving behind a cylindrical damaged zone few nanometers in diameter. Given the fact that this zone, the so-called latent track, exhibits much higher etch rates in hydrofluoric acid than the surrounding bulk, the authors arrived at a tapered profile with a round clean aperture 1–2 $\mu$m in diameter mimicking the internal profile of the patch micropipette, figure 4(*a*). Using such apertures, the authors successfully recorded from single artificial ion channels in bilipid membranes [41] and mammalian cells [43] (CHO, N1E-115). Rather routine formation of gigaseals (2–5 GΩ) on cells (CHO), however, was made possible by the constant improvements made to the technique [44]. Cells were self-positioned on the apertures automatically via a pressure/suction protocol. The device exhibited a fairly low capacitance (1 pF) and the currents from single-ion channels could be resolved in the cell-attached mode. The requirement of access to a heavy-ion accelerator and the necessity to carefully time the wet etching step happen to be major drawbacks of this approach. The alternative approaches subsequently developed managed to overcome such requirements as discussed below.

Wo and colleagues [45, 46] demonstrated funnel-like apertures on a cover glass through a $CO_2$ laser-based melt and reflow process which resulted in a smooth and debris-free surface similar to that produced by the heat-pulling and fire-polishing patch pipettes, figure 4(*b*). The funnel or hourglass profile of the aperture naturally guided a nearby cell to the aperture centre with the aid of slight suction. The authors reported a single gigaseal (1.9 GΩ) on a PC-12 cell (sample size unreported) using a 1-$\mu$m aperture while no gigaseal could be obtained on CHO cells as the seal resistances fell below 200 MΩ on average (out of 11 attempts). While the size variation across the apertures was not specified, the fabrication of 1–2 $\mu$m apertures was acknowledged to be a challenge due to variations in glass thickness and laser instability. Nevertheless, the authors managed to obtain gigaseals on CHO cells after having improved their technique by adopting a two-stage drilling process. The first stage applied pulses of relatively long duration generating abundant heat to put a hole in a cover slip of borosilicate glass 150 $\mu$m thick while the second stage immediately followed up with a series of short pulses to maintain moderate heating to have the molten glass reflow back into the aperture to stably reduce the diameter below 10 $\mu$m. The smallest size of the aperture obtained was roughly 2 $\mu$m. Using the apertures optimized in diameter 1–3 $\mu$m, the authors reported gigaseal success rates on HEK, CHO and Jurkat T lymphoma cells as 62.5%, 43.6% and 66.7%, respectively.

Blick and colleagues [82] raised particular interest in single crystal quartz as a patch substrate not only because of its low-noise characteristics but also because of its piezoelectric property. Quartz could provide a platform for nanomechanical stretching of a lipid bilayer membrane to study mechanosensitive ion channels. The authors adopted a fabrication method similar to laser-induced backside wet etching (LIBWE) [83] and demonstrated clean round apertures in borosilicate glass and single crystal quartz substrates. On

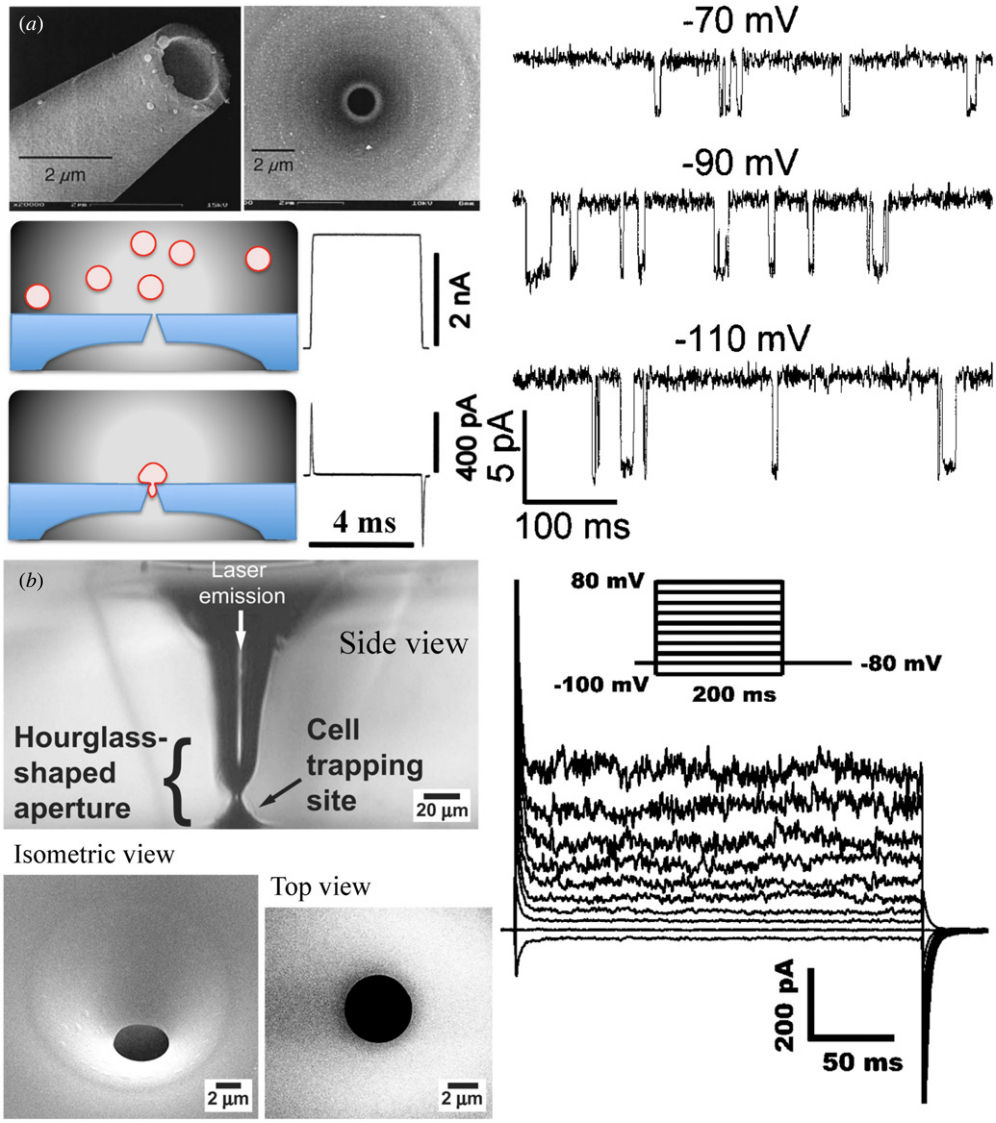


**Figure 4.** Planar designs in quartz/glass. (*a*) SEM images of the tip of a glass patch micropipette and an aperture (1 $\mu$m) ion-track etched into a quartz partition thinned down to 20 $\mu$m (upper left). The measured current across the etched aperture in response to a test pulse (10 mV) registered resistance values 4 MΩ and 5 GΩ before and after capturing a cell, respectively (lower left). Single-ion channels (BK-type $Ca^{2+}$-activated potassium channels) expressed in Chinese hamster ovary (CHO) cells recorded in a cell-attached configuration on the quartz chip at different holding potentials (right panel). (Adapted with permission from [44] and [43]. Copyright 2002, American Institute of Physics and Biophysical Society). (*b*) SEM images showing a representative aperture drilled in a cover glass by the $CO_2$ laser. Whole-cell current traces of endogenous channels in a HEK 293T cell recorded on the glass chip shown without leak subtraction. (Reprinted with permission from [46]. Copyright 2007, American Institute of Physics).

quartz, they reported low-noise recordings from Alamethicin channel proteins inserted in a lipid bilayer membrane secured on an aperture 25 $\mu$m in diameter with a stable gigaseal (>100 GΩ). In a later technique, [84] the authors managed to piezoelectrically tune the aperture size while monitoring Alamethicin channel activity demonstrating that the tension built up in the bilayer increases the probability of Alamethicin ion channels occupying larger conductance states. Patching mammalian cells on this platform would require smaller apertures down to 1–2 $\mu$m in diameter. Previously, the authors obtained apertures as small as 90 nm in diameter on thick glass or quartz substrates (150–300 $\mu$m) through a 'sandwich' drilling method [85]. However, no results on cells have been reported thus far using these apertures.

Heath and colleagues [47] fabricated ultra-smooth high-aspect ratio apertures in silicon dioxide and quartz films by a high-density plasma etching applied through a pore pattern in a Ni mask undercut beneath the overlaid photoresist pattern of smaller pores via electrochemical etching and polishing in a concentrated acid. The thickness of the Ni mask was shown to modulate the electric field within the dielectric film and thereby tuning the degree of ion bombardment to the aperture walls. Particularly, the wall smoothness was shown to increase with the thickness of the Ni mask. Smooth apertures 7–12 $\mu$m deep in fused quartz/silica with an initial resistance 0.8–3.0 MΩ delivered gigaseals on rat basophilic leukaemia (RBL) cells in nearly 80% of the attempts, with the majority from 20 to 80 GΩ. Such high performance was attributed to

the slightly inward tapered profile of the aperture, which might have favoured a more intimate contact with the cell membrane. On the contrary, no gigaseals could be obtained with shallower apertures as verified on those 0.5 $\mu$m deep in thermal oxide as well as those 1.5–5 $\mu$m deep in low-temperature oxide (LTO). No correlation was found between the yield of gigaseals and aperture diameter over a range of values studied (0.6–5.1 $\mu$m).

### *3.3. Polyimide*

Polyimide offers the advantage of being transparent while compatible with optical microscopy as well as cell culture. It is chemically and mechanically stable, has a low dielectric constant (∼3.5) and can be structured through standard microfabrication techniques. Stett and colleagues [33] demonstrated round patch apertures on a polyimide film 6.5 $\mu$m thick. The apertures had a nominal diameter 2 $\mu$m milled by a focused ion beam and 4 $\mu$m etched by $O_2$ plasma through a resist pattern. A $Si_3N_4$ film 100 nm thin was deposited to obtain a glass-like hydrophilic surface for enhanced seals. Attempts, however, returned fairly poor seals (<50 MΩ) with very rare encounter of gigaseals and whole-cell recordings on cardiac Purkinje cells and CHO cells. Despite the low seal quality, the authors were able to proceed with the loose-patch recordings of tetrodotoxin (TTX)-sensitive inward currents and recordings of action potentials in Purkinje cells.

Martinez and colleagues [48] created a pair of individually addressable apertures on a polyimide film 3 $\mu$m thick by reactive ion etching with $O_2$ plasma through a pattern of aluminium and photoresist mask. The apertures were 4 $\mu$m in diameter and, despite their large size, capable of registering gigaseals on the cardio-respiratory neurons of mollusc Lymnaea that were directly cultured on them for 2–4 h. The gigaseals were formed in 2 out of 12 apertures tested without having external suction or any other force applied while 4 apertures were found having already attained the whole-cell configuration. The authors further managed to record high-fidelity action potentials (neuronal activity) from the primary neurons cultured on these apertures.

### *3.4. Teflon*

Teflon is chemically stable and has excellent electrical properties: high resistivity ($>10^{18}$ Ω cm), low dielectric constant (∼2) and low dielectric loss factor ($\sim 2 \times 10^{-4}$). Apertures made in a thin Teflon partition are known to support planar lipid bilayers stable for several hours. However, the apertures smaller than 15 $\mu$m, let alone patch apertures, are usually difficult to achieve using conventional methods such as those involving mechanical punching, drilling, spark discharge burning, or shaving away backside of a sharp indentation on a sheet.

Whitesides and colleagues [86] fabricated apertures in amorphous Teflon (Teflon AF) sheets with chemical robustness comparable to standard Teflon while electrical and optical properties superior. The authors moulded apertures in this material from a template of sharp probe tip or patterned resist structures on a planar substrate. The conical-shaped apertures as small as 2 $\mu$m in a sheet 30 $\mu$m thick resulted from a metal probe tip with a diameter of 200 nm on hydrogel substrates. The apertures were applied for planar lipid bilayer experiments and those in diameter from 2 to 130 $\mu$m returned a mean seal resistance 258 GΩ. These apertures have yet to be demonstrated for cell-based experiments, which would require controlled and consistent fabrication of <2 $\mu$m apertures.

### *3.5. PDMS*

PDMS, a heat curable liquid resin, has become a popular soft polymer for prototyping microfluidics by replica moulding [87]. PDMS has many attractive attributes compared to other materials. Like Teflon, it has excellent electrical properties with a very low dielectric constant (∼2.5) and a low dielectric loss factor ($\sim 10^{-5}$). It is optically transparent and assumes a glass-like hydrophilic surface state once treated with oxygen plasma although this may not last long as it recovers its hydrophobic nature due to rearrangement of free silanol groups. It is more cost-effective than silicon in raw material. PDMS is also well known among patch-clamp scientists under the trade name Sylgard$^{TM}$ (Dow Corning) and routinely used as a coating layer to suppress glass micropipette noise. PDMS coating applied around the shank of a micropipette increases wall thickness in contact with bath solution while its hydrophobic nature stops the bath solution creeping up the wall [49].

Sigworth, one of the patch-clamp pioneers, and his colleagues discovered that patch pipette tips coated with PDMS readily form gigaseals if oxidized or else resist seal formation (<100 MΩ) [50]. Encouraged by the findings, they went on prototyping patch apertures in PDMS by replica moulding either from a quartz rod pulled into the shape of a patch pipette or from micromachined silicon pits. On oocytes, these apertures delivered gigaseals at a success rate of 13%, well below those achievable with the patch pipettes irrespective of PDMS coating (∼40%). The authors attributed the low success rates to the aperture geometry and size (4–20 $\mu$m). Later, by replicating smaller and round apertures (2$\mu$m) from a microstream of air, they nearly doubled the gigaseal success rate (25%) [51]. They managed to show whole-cell and cell-attached recordings from RBL-1 cells despite the lower gigaseal success rate they encountered with this cell type (∼10%). Whole-cell recordings from rat neuroblastoma cells were also reported with apertures replicated from the pipette-shaped rods. These studies, while they draw attention to PDMS and soft-lithography as an attractive substrate material and a convenient method of microstructuring, also hinted at the challenge of replicating in PDMS micron-size well-defined apertures with a planar design.

Luke Lee and colleagues demonstrated the first lateral design; a replica-moulded PDMS chip with apertures positioned on the sidewalls of a microchannel, figure 5(*a*) [65]. Referred to as lateral cell trapping junctions, the apertures are located at the intersection of fine microcapillaries and deeper microchannels. The authors used masters fabricated out of silicon with a dual-step profile; shallow features imparted by DRIE to define microcapillaries and tall features patterned

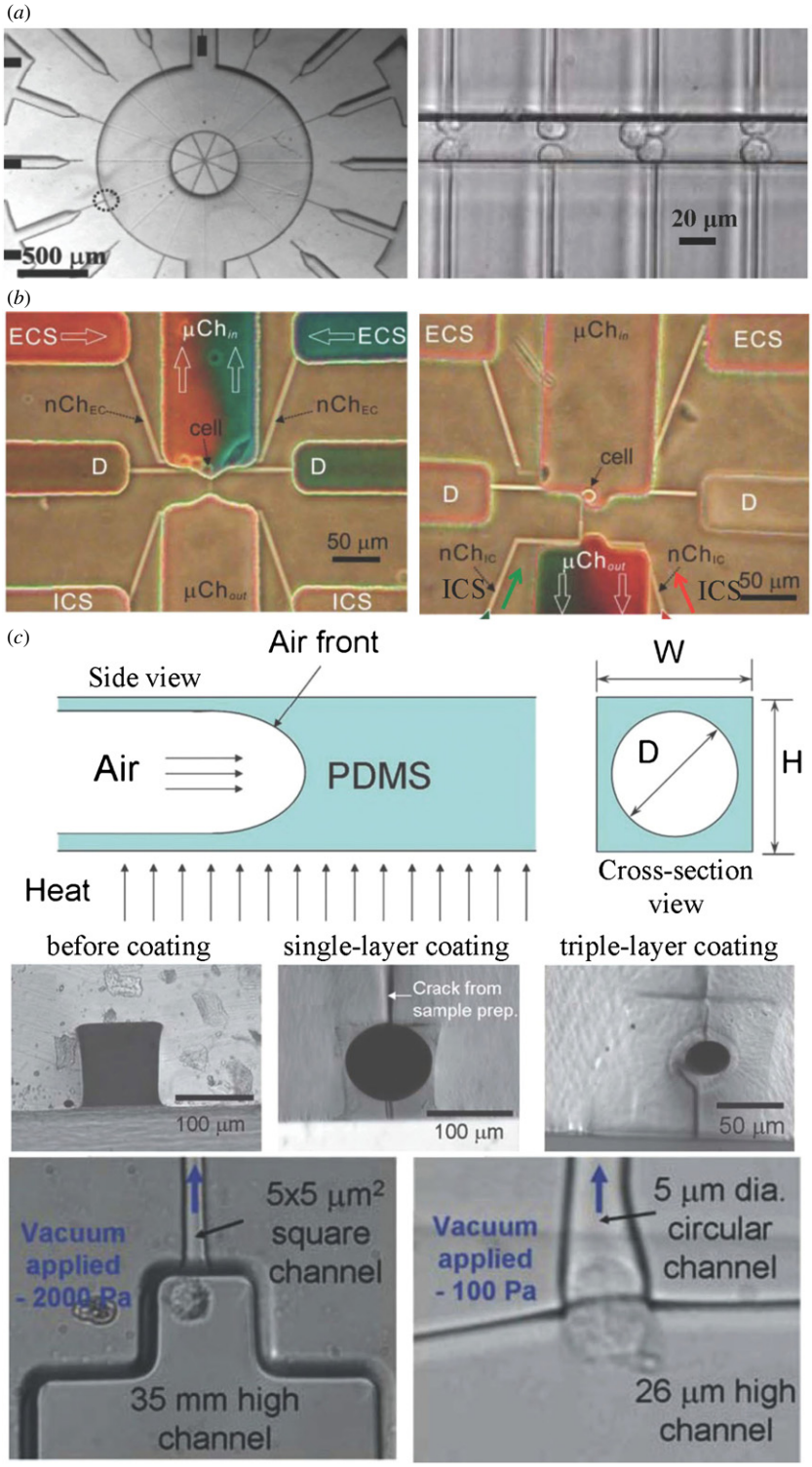


**Figure 5.** Lateral designs in PDMS. (*a*) Optical micrographs of a patch clamp array device with 14 radial patch channels (left) and of an array device with 8 linear patch channels (right), both shown from above. The latter demonstrates the utility of the patch apertures for selective placing of cell-pairs (fibroblasts) in membrane contact, enabling simultaneous optical characterization of direct cell–cell communication via gap junctions. (Adapted with permission from [65] and [75]. Copyright 2004 and 2005, American Institute of Physics). (*b*) Optical micrographs demonstrating the capability of a lateral design in leveraging microfluidics for rapid exchange of extracellular (ECS) and intracellular solution (ICS) while patching a cell. (Adapted with permission from [67]. Copyright 2006, The Royal Society of Chemistry). (*c*) Cross-sectional schematics describing shape transformation by a coating process whereby a rectangular microchannel filled with uncross-linked PDMS mixture is subjected to a constant supply of compressed air while rapidly cross-linking the PDMS coating under heat. SEM images of a 100 $\mu$m $\times$ 100 $\mu$m microchannel shown before and after the application of a single layer and triple layers of coating (centre). A vacuum pressure of $-2000$ Pa applied through a 5 $\mu$m $\times$ 5 $\mu$m rectangular microchannel is unable to trap a nearby SiHa cell (bottom left), while $-100$ Pa through a circular channel is sufficient to trap the cell (bottom right). (Adapted with permission from [89]. Copyright 2011, The Royal Society of Chemistry).

on thick SU8 resist to define deeper microchannels. They obtained apertures 3–4 $\mu$m in size and somewhat round due to light scattering artefact during lithography. The structures were bonded on a glass slide with a thin layer of PDMS coating leaving the apertures cornered between the sidewalls and the floor of the microchannel. Typical seal resistances obtained on human tumour cells (HeLa) were 140 MΩ on average and reached up to 200 MΩ. The structures displayed fairly low device capacitance (<1 pF) while exhibiting all the articulated virtues of the lateral configuration. Partial cure bonding [66], the technique later developed by the authors, led this type of apertures to reach gigaseals, albeit seldom (5%), and to deliver whole-cell recordings from mammalian cells (CHO). The authors did not specifically carry out $O_2$ plasma treatment to induce glass-like surface state that might have enhanced the seal statistics.

A subsequent study by Chihchen and Folch [67] applied $O_2$ plasma treatment on the lateral junctions in PDMS and reported an impressive success rate of nearly 60% on RBL-1 cells. During whole-cell recordings, the high stability of gigaseals allowed for solution exchange on both the extracellular and intracellular sides through integrated microcapillaries within 50 $\mu$m of the aperture, figure 5(*b*). This clearly demonstrated microfluidic integration as one of the key merits of a lateral design. The authors attributed the frequent encounter of gigaseals mainly to the enhanced topological definition of apertures replicated from resist patterns through high-resolution (electron-beam) lithography. Moreover, they failed to observe gigaseals without having surface exposure to $O_2$ plasma concurring with the findings of Sigworth and colleagues. Yet, they limited to an optimum exposure time of ∼6 min in comparison to 1–4 h as carried out by the other group [51]. It should be noted that cell trapping in a lateral design is typically achieved by suction applied through the aperture unlike many of the planar designs where cells are literally dropped on apertures.

One apparent drawback of lateral junctions compared to planar apertures is that the non-ideal aperture shape hinders tight seals. Although partially round apertures have been obtained through resist annealing or certain artefacts in mould fabrication, it would be more beneficial to attain a completely round aperture. Few authors demonstrated lateral junctions with round apertures. Weitz and colleagues [88] developed a technique whereby a sol-gel glass coating is applied on the walls of rectangular microchannels to increase their chemical resistance. Cylindrical microchannels emerged in the process when the glass coating under surface tension rounded off the channel corners. Although the apertures rather displayed a large diameter (>10 $\mu$m), the method, in principle, should allow smaller apertures for patching cells provided that the thickness of the coating applied can be controlled precisely. Sun and colleagues [89] subsequently demonstrated round apertures 5 $\mu$m in diameter by substituting sol-gel mixture with liquid PDMS and then constantly maintained a stream of compressed air supply to the microchannels during crosslinking the PDMS coating, figure 5(*c*). The method is somewhat similar to the air moulding technique introduced by Sigworth and colleagues [51] for forming planar patch apertures. The rounded aperture, unlike the rectangular counterpart of a comparable size, was shown to require much less effort to draw and trap a single cervical cancer cell (SiHa) although no report has been made on the seal quality achieved. Taking the advantage of the ability to visualize membrane deformations of single cells trapped at lateral junctions, the authors later on performed electrical and mechanical characterization of single cells using impedance spectroscopy and micropipette aspiration techniques on the same platform [90], albeit without the rounding benefit of the surface coating applied in liquid phase. In consequence, they encountered quite high leakage currents.

A further drawback of a lateral junction that may compromise the seal quality is the aperture location; the aperture is situated in direct contact with the bottom plane of the microchannel. This 'cornered' configuration keeps the aperture either entirely inaccessible to the cell or forces the cell to unnaturally deform to be able to reach the aperture and establish a contact. Lee and colleagues [68] addressed this concern with a revised design whereby the apertures are raised from the bottom by about 20 $\mu$m to give the cell enough room so that it does not have to undergo excessive deformation. The 'raised' apertures are situated on the sidewall of a large chamber that is open to the air as a result of macroscale punching in fabrication. This open platform, unlike the enclosed microfluidic chambers whereby the diffusion rate is typically limited by the low Reynolds number flow, allows more efficient fluidic exchange while introducing minimal perturbation to the seal quality. Although most seal resistances obtained on CHO and HEK cells remained less than 500 MΩ, the authors managed to obtain whole-cell configurations repeatedly at a success rate of ⩾80% and utilized their platform to characterize drug dose-response relation and drug binding activity.

### *3.6. Glass reflow on microstructured silicon*

In the pursuit of an ideal aperture for the lateral configuration, Yobas and colleagues [69] discovered self-enclosed cylindrical glass microcapillaries buried in narrow trenches in silicon. A layer of phosphosilicate glass (PSG), when deposited on a structured terrain such as a narrow trench, is folded over itself leaving a trapped void elongated inside the trench due to its non-conformal deposition [91]. The void exhibits a triangular cross-sectional profile initially but then evolves into a cylindrical microcapillary when allowed to undergo shape transformation in thermal anneal above the glass transition temperature (900–1100 °C) as described in figure 6. This leads to a fully round lateral aperture completely built in glass with a perfectly smooth surface owing to the thermal reflow process. Thermal reflow of PSG is a well-known planarization technique in integrated circuit manufacturing whereas the trapped voids are also encountered in isolation trenches between semiconductor devices due to incomplete filling and regarded as the 'keyhole' issue since they adversely affect the device reliability and performance [92]. Using the glass reflow technique, the authors demonstrated round lateral patch apertures ∼1.5 $\mu$m in diameter (variation <10%), and

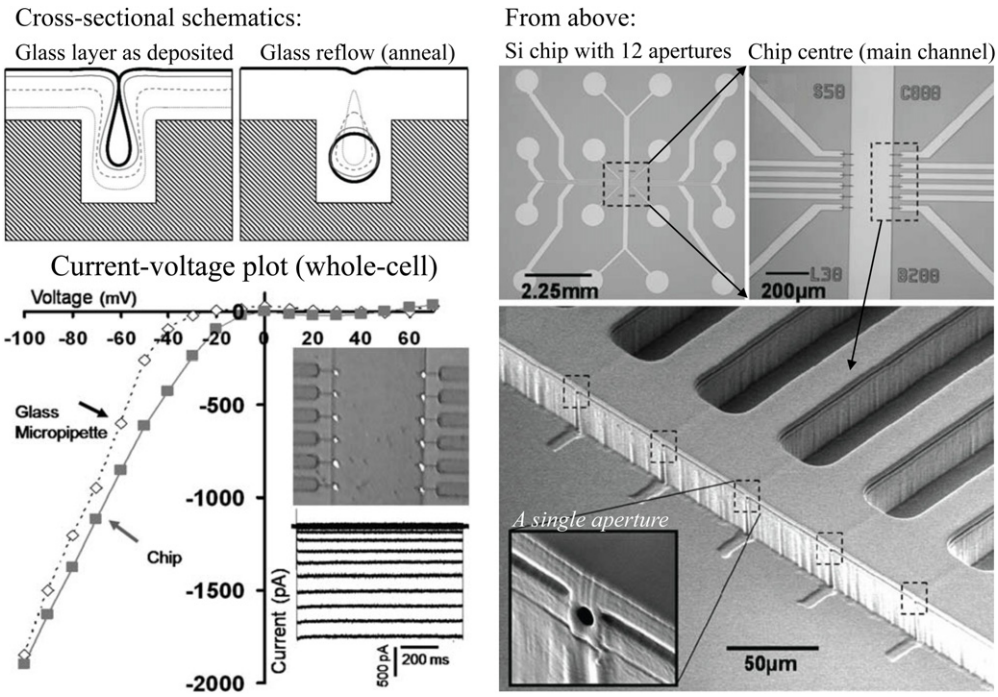


**Figure 6.** Lateral design in a doped glass layer formed upon thermal reflow on microstructured silicon. Conceptualized trench profiles in Si (upper left) describing the formation of a round patch aperture by enclosing a void in a partially filled trench due to non-conformal deposition of a doped phosphosilicate glass (PSG) and then shape transformation of the trapped void under glass reflow in thermal anneal. Photomicrographs of a design (upper right) that corresponds to a single unit of a 1536-well plate shown without the capping layer and featuring 12 patch apertures along the main channel fabricated through thermal reflow of glass. SEM image of a sidewall along the main channel posing round patch apertures (lower right). A current–voltage plot derived from whole-cell traces of endogenous potassium ion channels in RBL-1 cells with a strong inward rectification recorded through one of the patch apertures on the chip or a glass micropipette (lower left). (Adapted with permission from [70] and from [71]. Copyright 2006 and 2010, The Royal Society of Chemistry).

noted fairly high success rate in forming gigaseals on RBL-1 cells; 61 out of hundred attempts and of those 48% ended up with a whole-cell configuration [70]. The authors also verified drug activity by blocking macroscopic currents from inwardly rectifying $K^+$ channels through extracellular application of $Cs^+$. Moving towards a high-throughput assay, they built a single unit of a standard 1536-well plate with 4 × 4 wells offering dedicated access to lateral apertures (total 12) placed along a central microchannel in which cells suspension and drug reagents are delivered, see figure 6 [71]. Cells were captured at once blindly by suction applied irrespective of their proximity to the patch apertures, a more realistic scenario in high-throughput screening and yet revealed a serious washout issue with the cell suspension invading side channels supplying the patch apertures. This also resulted in a drastic decline in gigaseal statistics. To mitigate the issue, the authors subsequently revised the fluidic test protocol and proposed an alternative method of cell capture leveraging dielectrophoresis [93].

Lehnert and colleagues [39] subsequently applied the thermal reflow of PSG layer to their planar designs to generate a smooth surface around a silicon aperture etched into a funnel or nozzle shape. Since the purpose of the PSG reflow is to smoothen the surface of an existing aperture instead of moulding a new one, out of a trapped void, they needed to deposit a relatively thin PSG layer with a nominal thickness 1.5–2 $\mu$m while the duration of thermal anneal performed at 900–1100 °C appeared to be not that critical. The PSG layer also helped scaling the apertures down to 1 $\mu$m in diameter but only around the edge due to non-uniform sidewall coating. This profile imposed a fairly low access resistance while better emulating the tip opening of a glass patch pipette. Under good experimental conditions, the authors obtained gigaseals with the either aperture shape on wild-type non-adherent CHO cells in four out of ten attempts, while the remaining six returned seal levels from 50 to 230 MΩ. However, no whole-cell current was recorded probably due to the low-level expression of endogenous ion channels in wild-type CHO cells.

## 4. Integration considerations

Integration considerations take advantage of microfluidics to save on precious compounds and introduce functionality or automation in patch-clamp measurements. The utilization of microfluidics began in conventional settings whereby glass patch micropipettes are coupled with simple microfluidic perfusion systems for either rapid solution exchange or temperature control [94, 95]. Orwar and colleagues [94] introduced a chip-based microfluidic device that is mounted on a motorized stage to rapidly scan well-defined parallel streams on a single-cell being patched in an open volume at the end of a fixed glass micropipette. This platform provided a rapid exchange of local aqueous solution around the patched cell on the order of milliseconds to resolve kinetics of ion channels and their associated dose-response curve. The authors later

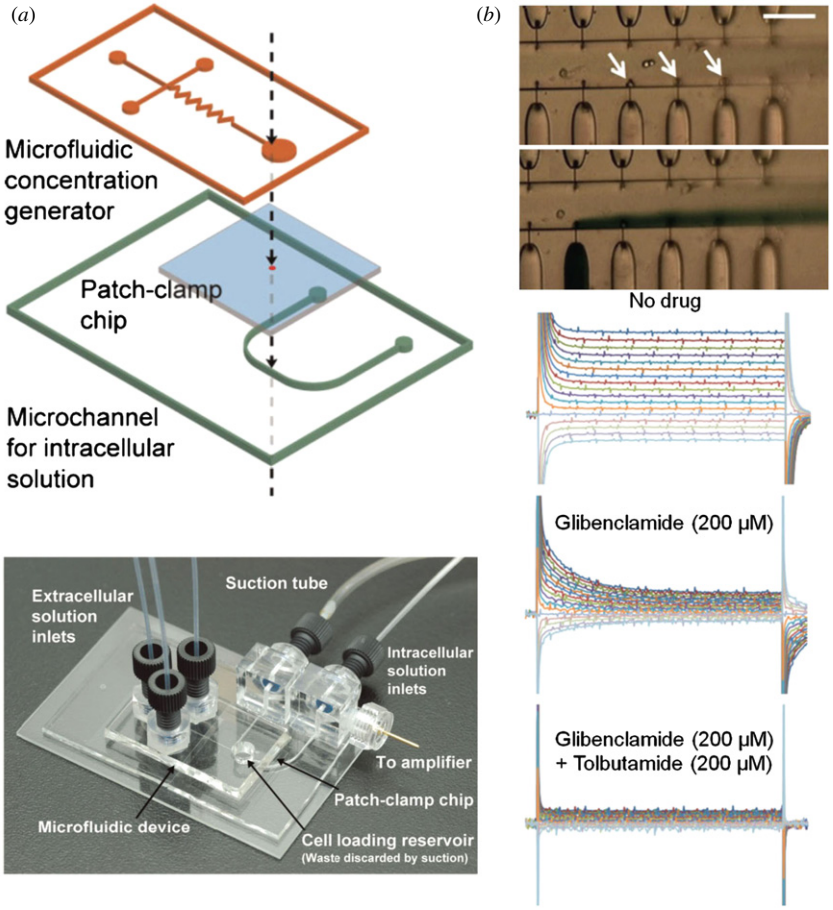


**Figure 7.** Microfluidic integration. (*a*) Planar design: a schematic of the proposed system outlining three key components aligned and assembled for on-demand generation of concentration profiles and their rapid exchange on patched cell (above). For a new measurement, the chip-to-chip integration allows one to readily replace the patch-clamp chip, a glass cover slip featuring a laser-drilled planar patch aperture. Picture of the assembled device. Adapted with permission from [98]. Copyright 2011, Wiley Periodicals, Inc. (*b*) Lateral design: photomicrographs of the main channel on a hybrid device (glass patch apertures on Si) featuring 12 individual apertures and their dedicated channels within a small field of view (scale bar 100 $\mu$m). Three cells (arrows) captured individually at the adjacent lateral apertures by suction applied to their respective access channels. The injection of a dye from one of the upstream channels visualizes the application of a drug compound on the cells captured downstream, while the constant flow of extracellular buffer in the main channel ensures the compound delivered to the cells without being diffused (below picture). Plots: whole-cell recordings of a voltage-gated potassium channel ($K_v$) activity from a rat insulinoma (INS-1) cell patched in the device while being exposed to sulfonylurea drugs. (Adapted with permission from [72]. Copyright 2012, Elsevier B. V).

integrated a microfluidic layout that can generate concentration gradients spanning nearly five orders of magnitude starting from a single concentration [96]. The platform was tested on voltage-gated hERG $K^+$ channels and ligand-gated GABAA receptors, providing highly resolved dose-response curves in less than 30 min that would have otherwise taken days to perform using conventional dilution and solution exchange.

Microfluidic integration of the planar designs involves further steps of fabrication (e.g. microchannel bonding over the patch aperture) and few groups thus far used microfluidics for directing cells to a planar patch aperture. Heath and colleagues [35] and later Matthews and Judy [36] assembled their micromachined silicon chips (processed via DRIE as described above) with PDMS flow-through microfluidics and demonstrated single cell alignment and positioning on the patch aperture. The latter group in their design also made a provision for a rapid fluid switching such that six distinct premixed compounds can be applied on the patched cell by flowing an alternating sequence of buffer and ligand plugs. Each aqueous plug was formed by a dedicated pair of offset microchannels crossing the main channel. However, poor seals obtained on cells prevented further use of such capability for dose-response measurements.

Sigworth and colleagues [97] employed microfluidics to multiplex a single recording channel of a patch clamp amplifier among multiple recording sites. The authors demonstrated a planar patch clamp array integrated with a microfluidic system comprising pneumatic microvalves built by multilayer soft lithography and allowed programmable electrofluidic isolation of the recording sites. The success rate of these valves in achieving the required isolation resistance ($>10$ G$\Omega$) was found to be more than 90%, albeit with a decrease in dc resistance over time possibly due to contamination after a few hours of stable operation. Disposable substrates containing individual planar patch apertures were reversibly mounted on the reusable system that contain eight parallel microvalves

integrated with thin-film Ag/AgCl electrodes. Each patch aperture mounted on the reusable system individually was micromoulded in PDMS using a micrometre-sized stream of nitrogen as reviewed earlier and bonded on a rather solid secondary support (glass slide) drilled with a hole. The authors tested the system on RBL-1 cells, achieving simultaneous whole-cell recordings with a gigaseal success rate in ∼28 out of 116 attempts. They also tested a small sample of glass chips containing ion-milled patch apertures and demonstrated gigaseals in 3 out of 19 attempts.

For the on-demand generation of compound concentrations and their rapid exchange on the patched cell, Wo and colleagues [98] integrated a microfluidic concentration generator with their planar patch clamp chip, a glass slide with a laser-drilled hourglass-shaped aperture, such that the glass slide can be easily replaced for the subsequent measurement as described in figure 7(*a*). The authors initially utilized a simple zigzag mixer design with two inputs to generate a linear concentration profile and demonstrated a series of experiments inclusive of recordings from volume-regulated chloride channels as well as voltage-gated potassium channels on HEK cells immersed in the generated streams expressing distinct osmolarities or drug concentrations. Excitation and then subsequent inhibition of ion channels was also demonstrated through a serial solution exchange on a single cell. Then the authors leveraged the same platform to derive dose-response curve by integrating a temporal logarithmic concentration generator [99], which is based on a serial dilution principle and controls the flow at each branching point through the design of fluidic resistances. Actuating different combination of valves, the authors dynamically altered the concentrations and performed dose–response assays on inhibitory activity of potassium channels on HEK cells by tetraethylammonium (TEA) solutions.

Leveraging microfluidics to generate a desired concentration profile and subsequently apply on the patched cell avoids the use of moving parts but nevertheless imposes certain limitations. Sample carryover between distinct compounds, particularly those hydrophobic, may be of a serious concern when the same microchannel is multiplexed among different compounds. Moreover, the possibility of losing small compound molecules to the chip material [100] due to adsorption casts some doubt on the accuracy of the concentration profile being applied to the patched cell and the dose-response curve derived. Furthermore, relatively large liquid body of an applied compound may get electrically coupled to the recording electrodes and induce large capacitive currents that may interfere with the measurements [98].

As for the lateral designs, they incorporate microchannels readily, owing to their inherent microfluidic integration. These microchannels can be utilized for various add-on functionalities. Several groups integrated auxiliary apertures adjacent to the patch apertures and had them dedicated to the manipulation and docking of cells to the patch apertures [68] and/or controlled delivery of test compounds on the patched cells [72, 74] under suction/pressure introduced. The former capability would be of a great value to maintain pristine patch

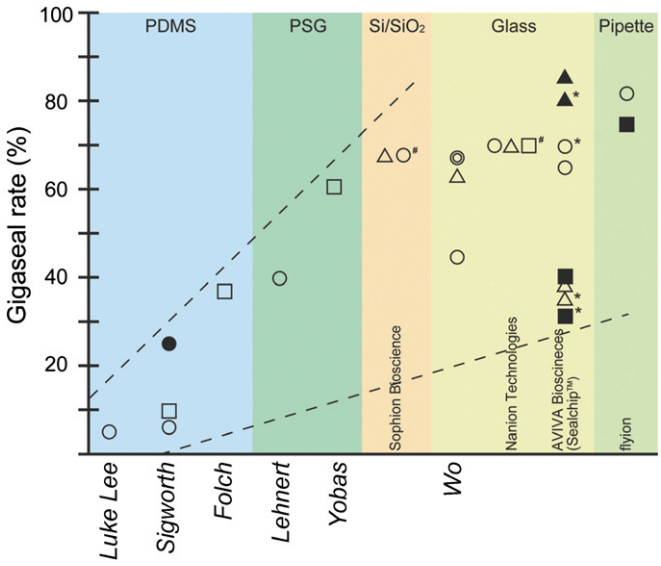


**Figure 8.** Gigaseal success rate among various technologies from research groups as well as companies. The chart is partitioned according to the substrate materials. The symbols denote the specific cell lines which the devices were characterized for: ◯ CHO, △ HEK, □ RBL, • Oocyte, ▲ Ltk, ■ CHL and ◎ Jurkat. (# Mean value calculated over a range and * accumax was applied for detaching cells rather than trypsin.) (Adapted with permission from [45]. Copyright 2009, The Royal Society of Chemistry).

apertures for an increased rate of occurrence of gigaseals while reducing the washout of the recording buffer [71]. The latter has been used recently by Bansal and colleagues in a hybrid device (glass patch apertures on Si) to apply drugs on the patched cells, figure 7(*b*). The authors employed the apertures upstream of the patched cells to deliver sulfonylurea drugs, a class of antidiabetics prescribed for managing Type-2 diabetes. Through whole-cell recordings from an insulin-secreting rat insulinoma (INS-1) cell, they showed partial and complete blockade of macroscopic currents from voltage-gated potassium channels ($K_v$) by perfusing the cell with glibenclamide alone or combined with tolbutamide. The same setup was also applied to showcase glucose dose responses of $K_v$ channels and the longevity of stable whole-cell recordings of $K_{ATP}$ channels that can be repeatedly elicited for up to 1 h without losing the gigaseal.

## 5. Conclusions and future outlook

More than a decade of extensive research has been devoted to the pursuit of microsystems for cell-based electrophysiology, particularly for the automation of skill-laden whole-cell patch clamp technique, leading to various approaches in design, microfabrication and integration as reviewed here. The level of success attained over the years can be seen in the performance of products from companies such as Sophion [52], Nanion [53, 54], Cytocentrics [55, 56], Molecular Devices (Ionworks [57–60] and PatchXpress [61, 62] featuring the technologies from Essen Instruments [57, 58] and the SealChip® [63] of Aviva Biosciences) and more recently Fluxion Biosciences [73]. As benchmarked in figure 8, some of these products return higher gigaseal success rates than those from academia

albeit with the underlying technical details proprietary, hence undisclosed. The products are known to cater distinct requirements: some offer medium throughput but high-quality recordings as a result of gigaseals attained while others relatively high throughput yet only maintain modest seals. For the latter, the so-called population patch clamp [59] has been devised whereby ensemble average of whole-cell recordings from a plurality of patch apertures in parallel (64 per well) is obtained. This is proven to address not only the issues with the modest values of seal resistance and the failure to obtain whole-cell configurations but also irregularities due to the variability of channel expression levels across cells. For the unoccupied apertures as well as those expressing poor seals, leak subtraction removes the linear leak current from the total measured to expose the nonlinear cellular ionic current. While all the products mainly target stable cell lines, which are induced to overexpress a particular type of ion channel, some of the products in recent years demonstrated the capability of patching stem cell-derived cardiomyocytes and neurons, cells from primary cultures and native cells such as human smooth muscle cells, neutrophils and lymphocytes [101–104]. These cells offer a more physiologically relevant expression system for ion channels.

While the majority of the studies concentrated on the planar approach, only few directed efforts towards the lateral design. Given the diversity of the devices with the planar configuration, the lateral design has not been fully explored, in part, due to the challenge in microfabricating a three-dimensional (lateral) patch aperture. This could be a deterrent if planar lithography is mostly what is left at our disposal. However, we believe that micro/nanofabrication is rich in techniques to circumvent such difficulty, as reflected in the lateral devices shown. To move forward, such devices, however, will have to address the 'corner' issue by repositioning their apertures away from the top and bottom confining boundaries. Still, this has to be done in a way that a reasonable aperture shape is maintained. A further issue to overcome is to manipulate a cell without resorting to excessive suction pressure through the aperture, which shall only be limited to draw the cell membrane in and/or break open the membrane.

Lastly, the idea of the inverted cell-pipette configuration whereby cells are manipulated to fixed patch apertures has been readily accepted by the most chip-based approaches. However, the impact of such inversion on the seal dynamics should not be underestimated. In the conventional settings, individual cells are typically patched, as they remain adhered to a solid support and their spreading affects the cell membrane. Even the cells of a non-adherent type can be more conveniently patched after the cells are plated on a glass cover slip with an adhesive coating (e.g. cell-Tac, poly-D-lysine, laminin) [105–108]. Suction applied through a nearby patch aperture draws in a portion of the cell membrane while the cell is pinned to the substrate. This configuration is certainly missing from many of the chip-based approaches and the absence of which might explain, at least in part, the frustratingly low success rate of gigaseal occurrence encountered in some of the studies despite their intricate patch apertures. Future experiments that can validate this hypothesis might shed light on the true characteristic of a successful design.

## Acknowledgments

This project was financially supported in part by the Startup Grant from the Department of Electronic and Computer Engineering, HKUST, and the Research Grant Council of Hong Kong, a Direct Allocation Grant to HKUST (grant no. DAG09/10.EG09).

## References

[1] Nicholls J G, Martin A R, Wallace B G and Fuchs P A 2001 *From Neuron to Brain* 4th edn (Sunderland, MA: Sinauer Association)
[2] Li S, Gosling M, Poll C T, Westwick J and Cox B 2005 *Drug Discov. Today* **10** 129–37
[3] Ashcroft F M 2000 *Ion Channels and Diseases: Channelopathies* (San Diego, CA: Academic)
[4] Aschroft F M 2006 *Nature* **440** 440–7
[5] Denyer J, Worley J, Cox B, Allenby G and Banks M 1998 *Drug Discov. Today* **3** 323–32
[6] Xu J, Wang X B, Ensign B, Li M, Wu L, Guia A and Xu J Q 2001 *Drug Discov. Today* **6** 1278–87
[7] Zheng W and Kiss L 2003 *Am. Pharm. Rev.* **6** 85–92
[8] Hammill O P, Marty A, Neher E, Sakmann B and Sigworth F J 1981 *Pflugers Arch.* **391** 85–100
[9] Hammill O P 1983 *Single-Channel Recordings* ed B Sakmann and E Neher (New York: Plenum) pp 451–71
[10] Asmild M *et al* 2003 *Receptors Channels* **9** 49–58
[11] Schnizler K, Kuster M, Methfessel C and Fejtl M 2003 *Receptors Channels* **9** 41–48
[12] Trumbull J D *et al* 2003 *Receptors Channels* **9** 19–28
[13] Owen D *et al* 2001 *Soc. for Neuroscience's 31st Ann. Meet. (San Diego, CA)*
[14] Owen D and Silverthorne A 2002 *Drug Discov. World* **3** 48–61
[15] Mathes C 2006 *Expert Opin. Ther. Targets* **10** 319–27
[16] Lepple-Wienhues A, Ferlinz K, Seeger A and Schafer A 2003 *Receptors Channels* **9** 13–17
[17] Kostyuk P G, Krishtal O A and Pidoplichko V I 1975 *Nature* **257** 691–93
[18] Wood C, Williams C and Waldron G J 2004 *Drug Discov. Today* **9** 434–41
[19] Sigworth F J and Klemic K G 2005 *IEEE Trans. Nanobiosci.* **4** 121–7
[20] Lehnert T and Gijs M A M 2007 *Lab-on-Chips for Cellomics: Micro and Nanotechnologies for Life Sciences* ed H Andersson and A van den Berg (Berlin: Springer) pp 143–69
[21] Behrends J C and Fertig N 2007 *Neuromethods* vol 38 2nd edn ed W Walz (Totowa, NJ: Humana) pp 411–33
[22] Fermini B 2008 *Top. Med. Chem.* **3** 1–25
[23] Dunlop J, Bowlby M, Peri R, Vasilyev D and Arias R 2008 *Nature Rev. Drug Discov.* **7** 358–68
[24] Farre C and Fertig N 2012 *Expert Opin. Drug Discov.* **7** 515–24
[25] Wang X B, Huang Y, Burt J P H, Markx G H and Pethig R 1993 *J Phys. D: Appl. Phys.* **26** 1278
Svoboda K and Block S M 1994 *Annu. Rev. Biophys. Biomol. Struct.* **23** 247–85
[26] Evander M, Johansson L, Lilliehorn T, Piskur J, Lindvall M, Johansson S, Almqvist M, Laurell T and Nilsson J 2007 *Anal. Chem.* **79** 2984–91
[27] Gijs M A M 2004 *Microfluid. Nanofluid.* **1** 22–40

[28] Nilsson J, Evander M, Hammarström B and Laurell T 2009 *Anal. Chim. Acta* **649** 141–57
[29] Demarche S, Sugihara K, Zambelli T, Tiefenauer L and Vörös J 2011 *Analyst* **136** 1077–89
[30] Zagnoni M 2012 *Lab Chip* **12** 1026–39
[31] Fertig N, Tilke A, Blick R H, Kotthaus J P, Behrends J C and Bruggencate G 2000 *Appl. Phys. Lett.* **77** 1218–20
[32] Schmidt C, Mayer M and Vogel H 2000 *Angew. Chem. Int. Ed.* **39** 3137–40
[33] Stett A, Bucher V, Burkhardt C, Weber U and Nisch W 2003 *Med. Biol. Eng. Comput.* **41** 233–40
[34] Sordel T, Garnier-Raveaud S, Sauter F, Pudda C, Marcel F, De Waard M, Arnoult C, Vivaudou M, Chatelain F and Picollet-D'hahan N 2006 *J. Biotechnol.* **125** 142–54
[35] Pantoja R, Nagarah J M, Starace D M, Melosh N A, Blunck R, Bezanilla F and Heath J R 2004 *Biosens. Bioelectron.* **20** 509–17
[36] Matthews B and Judy J W 2006 *J. Microelectromech. Syst.* **15** 214–22
[37] Lehnert T, Gijs M A M, Netzer R and Bischoff U 2002 *Appl. Phys. Lett.* **81** 5063–65
[38] Lehnert T, Laine A and Gijs M 2003 *Proc. μTAS 2003: 7th Int. Conf. of Miniaturized Chemical and Biochemical Analysis Syst. (Squaw Valley, CA)* pp 1085–88
[39] Lehnert T, Nguyen D M T, Baldi L and Gijs M A M 2007 *Microfluid. Nanofluid.* **3** 109–17
[40] Curtis J C, Baldwin K, Dworak B J, Stevenson J T M, Delivopoulos E, MacLeod N K and Murray A F 2008 *J. Microelectromech. Syst.* **17** 974–83
[41] Fertig N, Meyer C, Blick R H, Trautmann C and Behrends J C 2001 *Phys. Rev.* E **64** 040901
[42] Fertig N, George M, Klau M, Meyer C, Tilke A, Sobotta C, Blick R H and Behrends J C 2003 *Receptors Channels* **9** 29–40
[43] Fertig N, Blick R H and Behrends J C 2002 *Biophys. J.* **82** 3056–62
[44] Fertig N, Klau M, George M, Blick R H and Behrends J C 2004 *Appl. Phys. Lett.* **81** 4865
[45] Chen C Y, Tu T Y, Chen C H, Jong D S and Wo A M 2009 *Lab Chip* **9** 2370–80
[46] Chen C Y, Liu K T, Jong D S and Wo A M 2007 *Appl. Phys. Lett.* **91** 123901
[47] Nagarah J M, Paek E, Luo Y, Wang P, Hwang G S and Heath J R 2010 *Adv. Mater.* **22** 4622–27
[48] Martinez D, Py C, Denhoff M W, Martina M, Monette R, Comas T, Luk C, Syed N and Mealing G 2010 *Biomed. Microdevices* **12** 977–85
[49] Benndorf K 2009 *Single-Channel Recordings* 2nd edn ed B Sakmann and E Neher (New York: Springer) pp 129–45
[50] Klemic K G, Klemic J F, Reed M A and Sigworth F J 2002 *Biosens. Bioelectron.* **17** 597–604
[51] Klemic K G, Klemic J F and Sigworth F J 2005 *Pflugers Arch.* **449** 564–72
[52] Kutchinsky J *et al* 2003 *Assay Drug Dev. Technol.* **1** 685–93
[53] Brüggemann A, George M, Klau M, Beckler M, Steindl J, Behrends J C and Fertig N 2003 *Assay and Drug Dev. Technol.* **1** 665–73
[54] Brüggemann A, Stoelzle S, George M, Behrends J C and Fertig N 2006 *Small* **2** 840–6
[55] Stett A, Burkhardt C, Weber U, van Stiphout P and Knott T 2003 *Receptors Channels* **9** 59–66
[56] Scheel O, Himmel H, Rascher-Eggstein G and Knott T 2011 *Assay and Drug Dev. Technol.* **9** 600–7
[57] Schroeder K, Neagle B, Trezise D J and Worley J 2003 *J. Biomol. Screen.* **8** 50–64
[58] Kiss L, Bennett P B, Uebele V N, Koblan K S, Kane S A, Neagle B and Schroeder K 2003 *Assay Drug Dev. Technol.* **1** 127–35
[59] Finkel A, Wittel A, Yang N, Handran S, Hughes J and Costantin J 2006 *J. Biomol. Screen.* **11** 488–96
[60] Sorota S, Zhang X-S, Margulis M, Tucker K and Priestley T 2005 *Assay and Drug Dev. Technol.* **3** 47–57
[61] Tao H M *et al* 2004 *Assay Drug Dev. Technol.* **2** 497–506
[62] Dubin A E *et al* 2005 *J. Biomol. Screen.* **10** 168–81
[63] Xu J, Gula A, Rothwarf D, Huang M X, Sithiphong K, Ouang J, Tao G L, Wang X B and Wu L 2003 *Assay Drug Dev. Technol.* **1** 675–84
[64] Mills J P, Qie L, Dao M, Lim C T and Suresh S 2004 *Mech. Chem. Biosyst.* **1** 169–80
[65] Seo J, Ionescu-Zanetti C, Diamond J, Lal R and Lee L P 2004 *Appl. Phys. Lett.* **84** 1973–75
[66] Ionescu-Zanetti C, Shaw R M, Seo J, Jan Y N, Jan L Y and Lee L P 2005 *Proc. Natl Acad. Sci. USA* **102** 9112–17
[67] Chen C and Folch A 2006 *Lab Chip* **6** 1338–45
[68] Lau A Y, Hung P J, Wu A R and Lee L P 2006 *Lab Chip* **6** 1510–15
[69] Ong W L, Kee J S, Ajay A, Nagarajan R, Tang K C and Yobas L 2006 *Appl. Phys. Lett.* **89** 093902
[70] Ong W L, Tang K C, Agarwal A, Nagarajan R, Luo L W and Yobas L 2007 *Lab Chip* **7** 1357–66
[71] Tang K C, Reboud J, Kwok Y L, Peng S L and Yobas L 2010 *Lab Chip* **10** 1044–50
[72] Kongsuphol P, Bansal T, Tang K C and Fang K B 2012 *Sensors Actuators* B **173** 462–7
[73] Golden A P *et al* 2011 *Assay and Drug Dev. Technol.* **9** 608–19
[74] Sabounchi P, Ionescu-Zanetti C, Chen R, Karandikar M, Seo J and Lee L P 2006 *Appl. Phys. Lett.* **88** 183901
[75] Lee P J, Hung P J, Shaw R, Jan L and Lee L P 2005 *Appl. Phys. Lett.* **86** 223902
[76] Petersen K 1982 *Proc. IEEE* **70** 420–57
[77] Lärmer F and Schlip A 1996 *Patents* DE 4241045, US 5501893 and EP 625285
[78] Ayón A, Braff R, Lin C C, Sawin H H and Schmidt M A 1999 *J. Electrochem. Soc.* **146** 339–49
[79] Levis R A and Rae J L 1993 *Biophys. J.* **65** 1666–77
[80] Spierings G 1993 *J. Mater. Sci.* **28** 6261–73
[81] Li L, Abe T and Esashi M 2003 *J. Vac. Sci. Technol.* B **21** 2545–49
[82] Stava E, Yu M, Shin H C, Shin H, Rodriguez J and Blick R H 2012 *Lab Chip* **12** 80–7
[83] Wang J, Niino H and Yabe A 1999 *Appl. Phys.* A **68** 111–13
[84] Stava E, Yu M, Shin H C and Blick R H 2010 *IEEE Trans. NanoBiosci.* **9** 307–9
[85] Yu M, Kim H -S and Blick R H 2009 *Opt. Express* **17** 10044–49
[86] Mayer M, Kriebel J K, Tosteson M T and Whitesides G M 2003 *Biophys. J.* **85** 2684–95
[87] Duffy D C, McDonald J C, Schueller O J A and Whitesides G M 1998 *Anal. Chem.* **70** 4974–84
[88] Abate A R, Lee D, Do T, Holtze C and Weitz D A 2008 *Lab Chip* **8** 516–18
[89] Abdelgawad M, Wu C, Chien W-Y, Geddie W R, Jewettbe M A S and Sun Y 2011 *Lab Chip* **11** 545–51
[90] Chen J, Zheng Y, Tan Q, Zhang Y L, Li J, Geddie W R, Jewett M A S and Sun Y 2011 *Biomicrofluidics* **5** 014113
[91] Agarwal A, Nagarajan R, Ong W L, Tang K C and Yobas L 2008 *Sensors Actuators* A **142** 80–7
[92] Vassiliev V Y, Lin C, Fung D, Hsieh J and Sudijono J L 2000 *Electrochem. Solid State Lett.* **3** 80–3
[93] Luo Y, Cao X, Huang P and Yobas L 2012 *Lab Chip* **12** 4085–92
[94] Sinclair J, Pihl J, Olofsson J, Karlsson M, Jardemark K, Chiu D T and Orwar O 2002 *Anal. Chem.* **74** 6133–38
[95] Pennell T, Suchyna T, Wang J B, Heo J S, Felske J D, Sachs F and Hua S Z 2008 *Anal. Chem.* **80** 2447–51

[96] Pihl J, Sinclair J, Sahlin E, Karlsson M, Petterson F, Olofsson J and Orwar O 2005 *Anal. Chem.* **77** 3897–903
[97] Li X H, Klemic K G, Reed M A and Sigworth F J 2006 *Nano Lett.* **6** 815–19
[98] Chen C Y, Tu T Y, Jong D S and Wo A M 2011 *Biotechnol. Bioeng.* **108** 1395–403
[99] Chen C-Y, Wo A M and Jong D-S 2012 *Lab Chip* **12** 794–801
[100] Toepke M W and Beebe D J 2006 *Lab Chip* **6** 1484–86
[101] Milligan C J *et al* 2009 *Nature Protoc.* **4** 244–55
[102] Stoelzle S, Haythornthwaite A, Kettenhofen R, Kolossov E, Bohlen H, George M, Brüggemann A and Fertig N 2011 *J. Biomol. Screen.* **16** 910–16
[103] Stoelzle S, Obergrussberger A, Brüggemann A, Haarmann C, George M, Kettenhofen R and Fertig N 2011 *Front. Pharmacol.* **2** 1–11
[104] Estes D J, Memarsadeghi S, Lundy S K, Marti F, Mikol D D, Fox D A and Mayer M 2008 *Anal. Chem.* **80** 3728–35
[105] Egger M, Ruknudin A, Lipp P, Kofuji P, Lederer W J, Schulze D H and Niggli E 1999 *Cell Calcium* **25** 9–17
[106] Reuss L 2001 *J. Membr. Biol.* **179** 1–12
[107] Kokkinaki M, Sahibzada N and Golestaneh N 2011 *Stem Cells* **29** 825–35
[108] Liu L, Hansen D R, Kim I and Gilbertson T A 2005 *Am. J. Physiol. Cell Physiol.* **289** C868–80